

# Plasmonics: Engineering of highly confined electromagnetic modes

Stefan A. Maier

Centre for Photonics and Photonic Materials, Department of Physics,  
University of Bath, Bath BA2 7AY, UK, [S.Maier@bath.ac.uk](mailto:S.Maier@bath.ac.uk)

**Abstract:** *This conference proceedings paper presents a brief discussion of sub-wavelength electromagnetic energy localization using engineered coupled surface plasmon polariton modes occurring at metal/dielectric/metal three-layer stacks. Using a simple analytical model taking the energy in the metallic cladding layers into account, it is demonstrated that such heterostructures allow out-of-plane energy confinement below the diffraction limit. An application in the form of a metal nanoparticle plasmon waveguide operating via evanescent coupling of gap modes is presented, and conclusions for the general trade-off between localization and loss in plasmonic waveguiding drawn.*

## A condensed history of plasmonics

Plasmonics [1] is currently one of the major driving forces of the fascinating field of *nanophotonics*, which explores how electromagnetic fields can be confined over dimensions on the order of or smaller than the wavelength of light. It is based on interaction processes between electromagnetic radiation and conduction electrons at metallic interfaces or in small metallic nanostructures, leading to an enhanced optical near field of sub-wavelength dimension.

Research in this area demonstrates how a distinct and often unexpected behaviour can occur even with in bulk form well-characterized materials such as metals if discontinuities or sub-wavelength structure is imposed.

Another beauty of this field is that it is firmly grounded in classical physics, so that a solid background knowledge in electromagnetism is sufficient to understand main aspects of the topic.

However, history has shown that despite the fact that the two main ingredients of plasmonics - *surface plasmon polaritons* and *localized surface plasmons* – have been clearly described as early as 1900, it is often far from trivial to appreciate the interlinked nature of many of the phenomena and applications of this field. This is compounded by the fact that throughout the 20th century, surface

plasmon polaritons have been rediscovered in a variety of different contexts.

The mathematical description of these surface waves was established around the turn of the 20th century in the context of radio waves propagating along the surface of a conductor of finite conductivity [2, 3]. In the visible domain, the observation of *anomalous* intensity drops in spectra produced when visible light reflects at metallic gratings [4] was not connected with the earlier theoretical work until mid-century [5]. Around this time, loss phenomena associated with interactions taking place at metallic surfaces were also recorded via the diffraction of electron beams at thin metallic foils [6], which was in the 1960s then linked with the original work on diffraction gratings in the optical domain [7]. By that time, the excitation of Sommerfeld's surface waves with visible light using prism coupling had been achieved [8], and a unified description of all these phenomena in the form of surface Plasmon polaritons was established.

From then on, research in this field was so firmly grounded in the visible region of the spectrum, that several rediscoveries in the microwave and the terahertz domain took place at the turn of the 21st century, closing the circle with the original work from 100 years earlier. The history of *localized* surface plasmons in metal nanostructures is less turbulent, with the application of metallic nanoparticles for the staining of glass dating back to Roman times. Here, the clear mathematical foundation was also established around 1900 [9].

While there exist many recent reviews and introductions to the field, for example [10, 11], it is the purpose of this conference communication paper to briefly elucidate the general trade-off between localization and loss in plasmonics - highermode confinement implying larger fraction of the mode energy inside the metallic media, and therefore higher Ohmic losses. As an example, it is shown how the engineering of surface plasmon modes in metal/dielectric/metal heterostructures allows the excitation of gap-modes with good field confinement [12] while at the same time trying to keep losses due to Ohmic heating to a minimum. For this purpose, after a brief

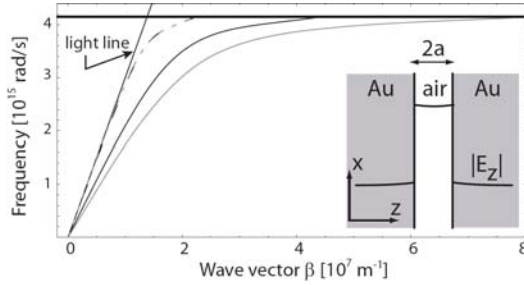


**FIG. 1:** Dispersion relation of the odd plasmon-polariton gap mode sustained by two infinite Au half spaces separated by an air gap  $2a$  (inset) for:  $2a = 1\ \mu\text{m}$  (broken black line),  $100\ \text{nm}$  (black line), and  $50\ \text{nm}$  (gray line). Also shown is the dispersion for a single interface (broken gray line). For large wave vectors, the frequency of the mode approaches the Au/air surface plasmon frequency (horizontal line).

discussion of how to assess subwavelength energy confinement, the specific example of a metal nanoparticle waveguide sustaining a mode preferentially localized in inter-particle gaps will be discussed. It is hoped that this will inspire more detailed investigations of the optimization between confinement and loss in a context of waveguiding using surface plasmons.

### The trade-off between localization and loss and gap-mode engineering

In order to investigate the ability of surface plasmons for sub-wavelength energy localization, we will as a didactic example study one of the simplest geometries of a multilayer structure, a thin dielectric layer (air) sandwiched between two metallic claddings (Fig. 1, inset).

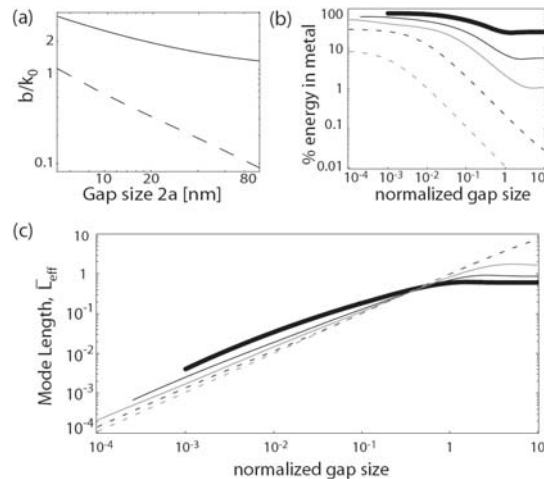
As is well known, such a heterostructure can support two surface modes propagating in the  $x$ -direction parallel to the interfaces that are set up by coupling of the surface plasmon-polariton modes of the individual air/metal boundaries [13]. Here the focus will be on the mode of odd *vector* parity, which does not have a cut-off gap size and shows a symmetric scalar field distribution of the dominant electric field component,  $E_z$ , with respect to the symmetry plane, as depicted in the inset of Fig. 1. The dielectric response of the metallic half-spaces is modelled using a Drude fit to the dielectric function  $\epsilon(\omega)$  for gold (Au) at visible and near-infrared frequencies [14]. More details regarding these and all subsequent calculations can be found in [12].

Fig. 1 shows the dispersion relation of the coupled mode for varying gap size  $2a$ . The dispersion for a single interface is also shown (broken gray line), which is seen to coincide with the dispersion for large gap sizes.

An important point to note here is that large propagation constants  $\beta$  can be achieved even for excitation significantly below the bulk metal plasma frequency provided that the gap width is chosen sufficiently small.

The ability to access such large wavevectors by adjusting the geometry indicates, as has been pointed out in previous work on sub-wavelength guiding structures [15], that localization effects that for a single interface can only be sustained at excitations near the material plasma resonance, can for this gap structure also be attained for excitation out in the mid- and far-infrared.

As will be seen below, this highly dispersive region of the bandstructure has a significant impact upon the effective size of the guided mode. Fig. 2(a) shows the evolution of both the real and imaginary parts of  $\beta$  with varying gap size for excitation at a free space wavelength of  $\lambda_0 = 850\ \text{nm}$ . Both parts are seen to increase with decreasing gap size, suggesting that the mode is becoming more electron-plasma in character, and that the electromagnetic energy is residing increasingly in the metal half-spaces. A plot of the fractional amount of energy inside the metal regions is shown in Fig. 2(b) for excitation at wavelengths  $\lambda_0 = 600\ \text{nm}$ ,  $850\ \text{nm}$ ,  $1.5\ \mu\text{m}$ ,  $10\ \mu\text{m}$ , and  $100\ \mu\text{m}$  ( $= 3\ \text{THz}$ ), reaching e.g. 40% for a gap of  $20\ \text{nm}$  at  $\lambda_0 = 850\ \text{nm}$ . For this and the following figure, the gap size is normalized to the



**FIG. 2:** (a) Normalized propagation constant  $\beta$  versus gap size at  $\lambda_0 = 850\ \text{nm}$ . Both the real (solid curve) and the imaginary (broken curve, 10x) part of  $\beta$  are seen to increase for decreasing gap. (b) Fractional electric field energy residing inside the metallic half spaces as a function of normalized gap size for excitation at  $\lambda_0 = 600\ \text{nm}$  (thick line),  $850\ \text{nm}$  (black line),  $1.5\ \mu\text{m}$  (gray line),  $10\ \mu\text{m}$  (broken black line), and  $100\ \mu\text{m}$  (broken gray line). (c) Effective mode length  $L_{\text{eff}}$  normalized to free space wavelength  $\lambda_0$ .

respective free space wavelength, and the results for each wavelength are plotted over the range of convergence of the analytical model.

It can be seen then, that along with the increased localization of the field to the metal/air interface, either via small gap sizes or excitation closer to the surface plasmon frequency, comes a shift of the energy into the metal regions.

### Electromagnetic energy density and the effective mode volume in plasmonics

It seems a natural question to ask if the effective size of the mode perpendicular to the metal/air interfaces drops below the diffraction limit if the energy pushed into the metallic half spaces with closing gap is considered properly. In order to get a better handle on the consequences of increasing fractions of the total energy of the mode entering the metallic cladding upon decreasing size of the dielectric gap, and to determine the overall effect on the scaling of the electric field strength per plasmon-polariton excitation in the air gap as a function of the gap size, one can define in analogy to the effective mode *volume*  $V_{\text{eff}}$  of cQED [16], an effective mode *length*  $L_{\text{eff}}$  for this one dimensional stack,

$$L_{\text{eff}}(z_0)u_E(z_0) = \int u_E(z)dz. \quad (1)$$

Here  $u_E(z)$  represents the electric field energy density at position  $z$ , with  $z_0$  corresponding to a position of interest within the cavity (usually the point of highest electric field strength). For the structure of Fig. 1,  $z_0$  resides in the air gap where an object may be placed to interact with the field. Fig. 2(c) shows the variation of  $L_{\text{eff}}$  (normalized to the free space wavelength  $\lambda_0$ ) with normalized gap size for the capacitor mode.

As can be seen, the mode lengths dropwell below  $\lambda_0/2$ , demonstrating that plasmonic metal structures do indeed sustain *effective* as well as *physical* mode lengths below the diffraction limit of light. The trend in  $L_{\text{eff}}$  with gap size tends to scale with the physical extent of the air gap. For large normalized gap sizes and low frequencies, this is due to the delocalized nature of the surface plasmon, leading to smaller mode lengths for excitation closer to the surface plasmon resonance frequency for the same normalized gap size. As the gap size is reduced to a point where the bandstructure of the capacitor mode turns over (see Fig. 1) and energy begins to enter the metallic half spaces, the continued reduction in mode length is due to an increase in field localization to the metal-air surface. In this regime, excitations with lower frequencies show smaller mode lengths

for the same normalized gap size than excitations closer to the plasmon resonance, due to the fact that more energy resides inside the metal for the latter.

This simple analysis of field confinement of surface plasmon modes can also be applied to surface plasmon polaritons propagating at a single interface, where confinement below the diffraction limit is possible only for frequencies that are a substantial fraction of the intrinsic surface plasma frequency of the conductor, and also for localized plasmons in metal nanoparticles.

### Waveguiding via interparticle gaps in linear nanoparticle chains

In the following, the concept of surface plasmon modes coupled via nanoscale dielectric gaps will be applied to a metal nanoparticle chain. Recently, there has been a huge amount of interest into the optical properties of metallic nanoparticles, due to the possibility of creating subwavelength modalities for confining and guiding light below the diffraction limit via the excitation of localized surface plasmons [11]. Specifically, it has been shown that one-dimensional arrays of closely spaced metallic nanoparticles can act as waveguides when excited at the dipole plasmon resonance frequency of the constituent particles [17]. The tight confinement offered by resonant excitation fundamentally implies substantial losses due to energy penetration into the metal and subsequent ohmic heating, leading to 1/e energy attenuation lengths below 1  $\mu\text{m}$ . Metal nanoparticle plasmon waveguides have thus far been analyzed via quasistatic models using generalized Mie-theory [18], point-dipole [19] and tight-binding [20] calculations, and by fully retarded models [21, 22] as well as finite-difference time-domain (FDTD) simulations [23]. Using these models, typical 1/e energy attenuation lengths between 750 and 900 nm have been estimated for arrays of 50 nm Ag spheres in air spaced by 25 nm gaps excited at the dipole particle plasmon frequency (corresponding to a free-space wavelength  $\lambda = 380$  nm). Nanoparticle plasmon waveguides operating using this principle have been fabricated and their guiding properties characterized using near-field optical microscopy [17]. The high confinement of optical energy offered by metal nanoparticle plasmon waveguides suggests applications for channelling energy to nano- and molecular scale detectors over modest distances, for example in a context of highly integrated optical sensing. However, tight confinement of the energy requires excitation at the dipole plasmon frequency of the constituent

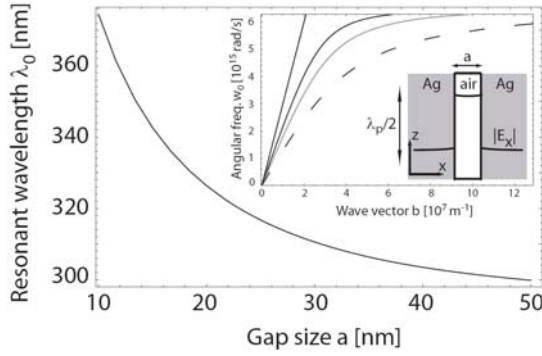


**FIG. 3:** Evolution of the wavelength of the fundamental gap resonance with gap width  $a$  for a Ag/air/Ag heterostructure (inset) calculated using a one-dimensional analytical model assuming perfect cavity mirrors confining the mode to a lateral size of 50 nm in the  $z$ -direction. The inset shows the dispersion relation of the coupled plasmon mode propagating in the  $z$ -direction for  $a=50$  nm, 25 nm, and 10 nm (black, grey and broken line, respectively).

particles, for which most of the energy of the mode resides in the particle itself, leading to high attenuation and only limited field accessibility. Additionally, resonant particle excitation constrains the tunability to longer wavelengths, which can only be achieved via increasing particle size or aspect ratio, or the refractive index of the surrounding host. For Ag nanoparticles, this leads to a broadening of the dipole resonance due to retardation effects and radiative losses, adversely affecting the guiding properties. While waveguides operating on this resonant particle principle have been successfully fabricated and characterized [17], this guiding mechanism cannot readily explain the experimental observation of a lower electric field distribution above the particles compared to the interparticle gaps obtained using collection mode near-field optical microscopy [24].

To overcome this discrepancy and enlarge the versatility of plasmon waveguides, here a new design principle for metal nanoparticle plasmon waveguides is presented that overcomes the requirement of resonant excitation of the particle plasmon while additionally maximizing the amount of energy outside the particles themselves. High confinement of the electromagnetic energy is assured via the excitation of evanescently coupled resonant modes in the gaps between adjacent particles. Adjustment of the gap dimensions (width and lateral size) allows for a tuning of the guiding frequency, mode size as well as attenuation length (via the quality factor of the fundamental gap resonance). Regarding the later,

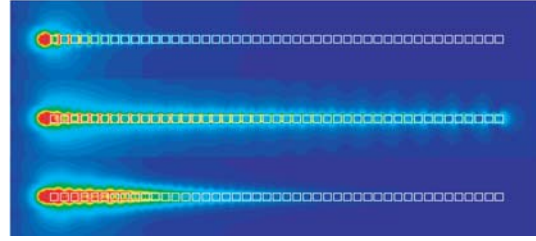


**FIG. 4:** Electric field distribution around nanoparticle plasmon waveguides excited using a longitudinally polarized point-dipole located to the left of the waveguide at  $\lambda_0=500$  nm (top), 429 nm (center), and 390 nm (bottom). In the case of resonant excitation at 429 nm, the energy is efficiently guided along the array. The color scale spans 5 orders of magnitude in the absolute value of the electric field

the amount of energy inside the metal particles and thus the attenuation is determined by the size of the gap, allowing relatively low-loss operation via careful tuning of the ratio between the evanescent coupling in the air and metallic regions, respectively.

In the following, Ag cubes of dimensions  $50 \times 50 \times 50$  nm $^3$  in air spaced by a gap of size  $a$  will be considered as the fundamental building blocks of a plasmon waveguide. Before presenting results obtained from three-dimensional FDTD simulations, the nature of the fundamental mode squeezed in the nanometric space between two metal particles can best be analyzed using the simple, one-dimensional analytical model of a metal/air/metal heterostructure presented above employing a straightforward boundary condition analysis.

The inset of Fig. 3 shows the dispersion relation for this mode for gap sizes of 50 nm (black line), 25 nm (grey line) and 10 nm (broken line), respectively. As can be seen, the real part of the propagation constant of the mode along the interfaces increases for decreasing gap size, leading to a reduced wavelength of the propagating plasmon  $\lambda_p = 2\pi/\beta$ . Thus, the wavelength of the propagating plasmon can be tuned via the size of the gap, which additionally controls the amount of dissipation due to the fact that upon decreasing gap the fraction of the energy of the mode inside the metallic half-spaces increases.

This structure can be converted into a Fabry-Perot type resonator by inserting perfectly reflecting cavity walls perpendicular to the direction of propagation. Thus, the fundamental mode will be excited when the cavity length  $d$  equals  $\lambda_p/2$ . Figure 3 shows the evolution of the corresponding free-space wavelength of excitation  $\lambda_0$  with gap

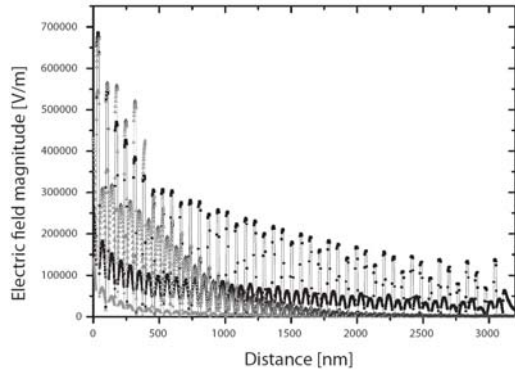


**FIG. 5:** Magnitude of the electric field along the waveguide axis for excitation at 500 nm (grey circles), 429 nm (black squares), and 390 nm (open triangles). After a fast initial decay due to transient effects, relatively low-loss guiding with a  $1/e$  field decay of  $\alpha_F^{-1} = 2200$  nm occurs for resonant excitation at 429 nm.

size for a fixed cavity length  $d=50$  nm. As expected,  $\lambda_0$  increases for decreasing gap size due to the increase in the wave vector  $\beta$  of the fundamental mode. Thus, there exists an intricate interdependency between gap size, cavity length, resonant wavelength and attenuation of the two-dimensional cavity.

The proposed plasmon waveguide relies on the evanescent coupling of adjacent gaps separated by a metallic nanoparticle, which was analysed using FDTD simulations of a chain of 45 Ag nanoparticles spaced by a gap of size  $a=20$  nm. The first particle was excited using a dipole oriented along the waveguide axis. Using pulsed excitation, the resonant frequency of the fundamental gap mode was determined to  $7 \times 10^{14}$  Hz, corresponding to  $\lambda_0 = 429$  nm. The resonant wavelength is longer than that predicted (325 nm) using the simple one-dimensional model with perfectly reflecting cavity boundaries, which is due to the field penetration into the air-space surrounding the particles, thus increasing the resonant wavelength. Fig. 4 shows the absolute value of the electric field on a linear color scale for excitation at 500 nm (top), 429 nm (center), and 390 nm (bottom). Clearly, significant guiding along the waveguide takes place upon resonant excitation only. Additionally, the field is seen to be tightly confined inside the gap regions in agreement with the squeezed near-field observed in [25], while in the particles themselves the electric field is confined to the surfaces, as opposed to the homogeneous polarization sustained during dipole particle plasmon excitation of spherical nanoparticles. In the latter case, excitation of longitudinally coupled dipolar modes

show some resemblance to the gap modes presented here for cubic particles, however with larger penetration of the electromagnetic fields inside the metal nanoparticles.

Fig. 5 shows the absolute value of the electric field along the waveguide axis through the particle centers for the three wavelengths of interest. While nonresonant excitation is characterized by a rapid decrease in field amplitude after only a small number of gaps, for resonant excitation relatively low-loss guiding is seen to be possible. In this case, a number of interesting features are apparent. Firstly, at the beginning of the waveguide close to the excitation source, an initial fast decay of the field over the first 6 gaps is apparent, which can be attributed to transient effects and direct excitation from the source at a distance. The same phenomenon was previously seen in plasmon waveguides excited at the particle plasmon resonance frequency [21]. Additionally, towards the end of the waveguide modulating effects due to the reflection of the guided wave at the impedance mismatch after the last particle are discernable. Incorporating the effects of this reflection, an exponential decay of the electric field amplitude along the waveguide with a decay constant  $\alpha_F^{-1} = 2200$  nm was determined, corresponding to a  $1/e$  energy attenuation length  $\alpha_E^{-1} = 1100$  nm. To verify the exponential decay fits, waveguides with varying number of particles have been simulated, yielding close agreement in their attenuation lengths.

Thus, metal nanoparticle plasmon waveguides guiding electromagnetic energy via coupled gaps compare reasonably favourably to the dipole particle plasmon case in terms of field accessibility and also energy attenuation. Additionally, the number of variables available (particle size, gap size, gap width) for tuning the excitation wavelength should allow for the design of plasmon waveguides tailored for particular applications. From a practical standpoint, gap widths on the order of 20 nm are possible using top-down fabrication techniques such as electron beam lithography or ion-beam milling.

Results obtained for the influence of substrates and dielectric hosts will be presented elsewhere, together with an extended study of the dependency of the energy attenuation length on particle and gap size.

## Conclusion

In summary, the ability to confine electromagnetic energy to mode sizes well below the diffraction limit has been elucidated via a discussion of gap

modes in metal/dielectric/metal heterostructures. This concept can be applied in a context of waveguiding using arrays of closely spaced metallic nanoparticles. The excitation of resonant gaps instead of particles increases the amount of tunability of plasmonic waveguides and compares favourably in terms of energy attenuation while at the same time providing highly localized and accessible fields, promising useful applications for a subwavelength photonic sensing and guiding infrastructure.

Clearly, the examples presented in this paper can serve only as a starting point for detailed investigations into waveguide geometries with the most favorable confinement/loss trade-off. A more detailed investigation of this issue will be necessary in order to assess the potential of plasmonics to be of importance for emerging technologies of highly miniaturized optical circuits or on-chip data communication.

### Acknowledgements

This work was sponsored by the Engineering and Physical Sciences Research Council EPSRC.

### References

- [1] S. A. Maier, M. L. Brongersma, P. G. Kik, S. Meltzer, A. A. G. Requicha, and H. A. Atwater, *Adv. Mat.* **13**, 1501 (2001).
- [2] A. Sommerfeld, *Ann. Phys. und Chemie* **67**, 233 (1899).
- [3] J. Zenneck, *Ann. d. Phys.* **23**, 846 (1907).
- [4] R. W. Wood, *Proc. Phys. Soc. London* **18**, 269 (1902).
- [5] U. Fano, *J. Opt. Soc. Am.* **31**, 213 (1941).
- [6] R. H. Ritchie, *Phys. Rev.* **106**, 874 (1957).
- [7] R. H. Ritchie, E. T. Arakawa, J. J. Cowan, and R. N. Hamm, *Phys. Rev. Lett.* **21**, 1530 (1968).
- [8] E. Kretschmann and H. Raether, *Z. Naturforschung* **23A**, 2135 (1968).
- [9] G. Mie, *Ann. Phys.* **25**, 377 (1908).
- [10] W. L. Barnes, A. Dereux, and T. Ebbesen, *Nature* **424**, 824 (2002).
- [11] S. A. Maier and H. A. Atwater, *J. Appl. Phys.* **98**, 011101 (2005).
- [12] S. A. Maier, *Opt. Express* **14**, 1957 (2006).
- [13] B. Prade, J. Y. Vinet, and A. Mysyrowicz, *Phys. Rev. B* **44**, 13556 (1991).
- [14] P. B. Johnson and R. W. Christy, *Phys. Rev. B* **6**, 4370 (1972).
- [15] J. Takahara, S. Yamagishi, H. Taki, A. Morimoto, and T. Kobayashi, *Phys. Rev. B* **22**, 475 (1997).
- [16] L. C. Andreani, G. Panzarini, and J.-M. Gerard, *Phys. Rev. B* **60**, 13276 (1999).
- [17] S. A. Maier, P. G. Kik, H. A. Atwater, S. Meltzer, E. Harel, B. E. Koel, and A. A. G. Requicha, *Nat. Mat.* **2**, 229 (2003).
- [18] M. Quinten, A. Leitner, J. R. Krenn, and F. R. Aussenegg, *Opt. Lett.* **23**, 1331 (1998).
- [19] M. L. Brongersma, J. W. Hartman, and H. A. Atwater, *Phys. Rev. B* **62**, R16356 (2000).
- [20] S. Y. Park and D. Stroud, *Phys. Rev. B* **69**, 125418 (2004).